Journal of Applied Mathematics and Physics, 2026, 14(6), 2409-2427
https://www.scirp.org/journal/jamp
ISSN Online: 2327-4379
ISSN Print: 2327-4352

Linearly Varying Deceleration Parameter with Axion Dark Matter in $f(R,T)$ Gravity

Sachin Pralhadrao Hatkar[1], Gajanan Dattarao Karhale[2], Dnyaneshwar Pralhad Tadas[3*], Shivdas Devmanrao Katore[4]

[1]Department of Mathematics, A.E.S. Arts, Commerce and Science College, Hingoli, India
[2]Department of Mathematics, Shankarrao Patil Mahavidyalaya, Bhoom, India
[3]Department of Mathematics, Toshniwal Arts, Commerce and Science College, Sengaon, India
[4]Department of Mathematics, Sant Gadge Baba Amravati University, Amravati, India
Email: *dtadas144@rediffmail.com

How to cite this paper: Hatkar, S.P., Karhale, G.D., Tadas, D.P. and Katore, S.D. (2026) Linearly Varying Deceleration Parameter with Axion Dark Matter in $f(R,T)$ Gravity. *Journal of Applied Mathematics and Physics*, **14**, 2409-2427.
https://doi.org/10.4236/jamp.2026.146118

Received: May 22, 2026
Accepted: June 21, 2026
Published: June 24, 2026

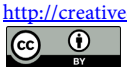

Abstract

In this paper, we have investigated the flat FLRW spacetime with axion dark matter in the context of $f(R,T)$ theory of gravitation. The solution of the field equation is obtained by using linear varying deceleration parameter. It is observed that the universe was decelerated in the past and accelerated at present. Also, the energy conditions and State finder pair $\{r,s\}$ are analyzed in details.

Keywords

FLRW Metric, Axion Dark Matter, $f(R,T)$ Gravity

1. Introduction

Recent astronomical observations, such as those of Type Ia supernovae with large redshift and measurements of cosmic microwave background (CMB) anisotropic, strongly suggest that the universe is undergoing an accelerated expansion [1]-[4]. This unexpected acceleration cannot be fully explained by Einstein's General Relativity (GR) combined with ordinary matter and has led to the introduction of dark energy (DE), a mysterious form of energy that constitutes about 73% of the total energy content of the universe. One favorable candidate for dark energy is axion dark matter, which derived from axions and initially suggested in particle physics to fix the strong CP problem in quantum chromodynamics (QCD). When these axions are very light and move slowly, they can behave like quintessence a dynamic scalar field responsible for the negative pressure providing cosmic accel-

eration. In this reference, axions are modeled using a scalar field with a periodic potential, usually resembling a cosine function, which evolves slowly over cosmic time and generates repulsive pressure counteracting gravitational attraction, thus accelerating the expansion of the universe.

To better explain this acceleration and go after the restrictions of GR, several modified theories of gravity have been introduced such as the $f(R)$, $f(G)$, $f(R,G)$, $f(T)$ and $f(R,T)$ [5]-[9] etc. The $f(R)$ theory of gravity is derived by substituting the Ricci scalar R in Einstein–Hilbert action with a general function $f(R)$. This theory first explored by Buchdahl [5]. $f(R)$ theory is further expanded to $f(R,T)$ theory of gravitation, which is presented by Harko *et al*. [8]. In this framework, the gravitational Lagrangian is a function of both the Ricci scalar R, which compact curvature due to gravity, and the trace T of the energy-momentum tensor, which contain the effect of matter and energy. This coupling between matter and geometry permit $f(R,T)$ gravity to include quantum effects and matter-geometry actively more naturally than general relativity. At first, the $f(R,T)$ theory universalize the well-known $f(R)$ gravity and yield a more workable and practical model of the universe's evolution. It has shown strong potential in modeling not only the late-time acceleration of the universe but also other cosmological phenomena such as transitions between different phases of expansion, the presence of introduced structures like wormholes, and the behavior of compact astrophysical objects.

In the cosmological reference, $f(R,T)$ gravity has shown effective in simulating cosmic acceleration without requiring a clear dark energy component, making it very suitable for integrating scalar fields like axion dark matter. Several studies have introduced the evolution of the universe in $f(R,T)$ gravity under different cosmological scenarios, including anisotropic models and Bianchi type metrics. Houndjo [10] has discussed the transition from a matter dominated phase to an accelerated phase in the $f(R,T)$ gravity. The case of perfect fluid for the Bianchi type III in $f(R,T)$ is investigated by Reddy *et al*. [11]. Moraes [12] has presented unification of the Kaluza-Klein extra-dimensional model with the $f(R,T)$ gravity. Azizi [13] investigated the wormhole solutions in the background of $f(R,T)$ gravity. Elizalde and Khurshudyan [14] investigated the models for static wormholes in the framework of $f(R,T)$ gravity. Banerjee *et al*. [15] studied the static spherically symmetric wormhole structures sustained by the isotropic matter sources in $f(R,T)$ gravity.

Thus, in this work, we discuss a cosmological model in $f(R,T)$ gravity with flat FLRW line element by introducing axion dark matter and a linearly varying deceleration parameter (LVDP), which facilitates a smooth evolution from the deceleration to acceleration phase in the evolution of the universe. This together offers a mathematically advanced and meaningful setting to study the accelerated expansion of the universe from a mathematical point of view.

The paper is organized as follows: Section 2 deals with metric and field equations. In Sections 2.1 and 2.2, we used the linearly varying deceleration parameter

to solve the $f(R,T)$ gravity field equations. Section 3 is devoted to the analysis of state-finder pairs. The energy conditions are presented in Section 4. The last Section 5, is devoted to summarizing obtained results.

2. Metric and Field Equation

The flat Friedmann-Lemaitre-Robertson-Walker (FLRW) models are the best for describing the current large-scale structure of the universe. The homogeneous and isotropic nature of the FLRW model plays an important role in understanding the origin of the universe. We have considered the flat FLRW spacetime as

$$\mathrm{d}s^2 = -\mathrm{d}t^2 + a^2(t)\left(\mathrm{d}x^2 + \mathrm{d}y^2 + \mathrm{d}z^2\right) \tag{1}$$

where $a(t)$ is a scale factor. Recently, Pradhan *et al.* [16] have studied dark energy behavior of the flat FLRW universe with viscous fluid in $f(Q)$ theory of gravity. The energy momentum tensor of perfect fluid is given as

$$T_{ij} = (\rho_t + p_t)\mu_i\mu_j - p_t g_{ij} \tag{2}$$

Here μ_i is the four-velocity of the fluid's with components $(0,0,0,1)$ satisfying $\mu_i\mu^i = 1$, ρ_t is the total energy density of the fluid, p_t is the isotropic pressure of the fluid. The equation of state (EoS) of a perfect fluid is $p = \gamma\rho$ with $\gamma \in [0,1]$ where ρ, p are the energy density and pressure of matter respectively.

We discuss the case of modified gravity $f(R,T)$. A generalization of $f(R)$ is $f(R,L_m)$ where coupling of matter Lagrangian and of the Ricci scalar was proposed by Bertolami *et al.* [17]. Coupling of matter and geometry is well described in $f(R,T)$ gravity. It allows matter and geometry to be arbitrary function of T and of R.

The action of $f(R,T)$ is given by Harko *et al.* [8]

$$S = \frac{1}{16\pi}\int f(R,T)\sqrt{-g}\,\mathrm{d}^4x + \int L_m\sqrt{-g}\,\mathrm{d}^4x \tag{3}$$

where L_m is matter Lagrangian density, and $f(R,T)$ is arbitrary function of Ricci scalar R and the trace T of T_{ij}. All other symbol have their usual meaning in $f(R,T)$ theory of gravity. By varying the action (3) with respect to metric g_{ij}, we can derive field equations of the $f(R,T)$ gravity model as

$$\begin{aligned} &f_R(R,T)R_{\mu\nu} - \frac{1}{2}f(R,T)g_{\mu\nu} + \left(g_{\mu\nu}\nabla^\mu\nabla_\nu - \nabla^\mu\nabla_\nu\right)f_R(R,T) \\ &= 8\pi T_{\mu\nu} - f_T(R,T)T_{\mu\nu} - f_T(R,T)\Theta_{\mu\nu} \end{aligned} \tag{4}$$

where $f_R(R,T) = \dfrac{\partial f(R,T)}{\partial R}$, $f_T(R,T) = \dfrac{\partial f(R,T)}{\partial T}$, ∇_μ is operator for covariant derivative. Field equations are depends on $\Theta_{\mu\nu}$. Here, we choose $L_m = -p_t$ which gives $\Theta_{\mu\nu} = -2T_{\mu\nu} - p_t g_{\mu\nu}$. It should be note that $f(R,T)$ is arbitrary function of R and T, therefore, different models of $f(R,T)$ gravity are possible for choice of R and T. Singh and Singh [18] have chosen the functional form $f(R,T) = R + 2f_1(T)$ to explore field equations. Here, we consider the following general form of the functional $f(R,T)$ proposed by Harko *et al.* [8]:

$$f(R,T) = f_1(R) + 2f_2(T) \tag{5}$$

here, $f_1(R) = R$ and $f_2(T) = \mu T$, where μ is constant.

The field equation for line element (1), using Equations (4), (5) and (2) takes the form

$$2\dot{H} + 3H^2 = (8\pi + 3\mu)p_t - \mu\rho_t \tag{6}$$

$$3H^2 = -(8\pi + 3\mu)\rho_t + \mu p_t \tag{7}$$

with

$$p_t = p + p_a, \quad \rho_t = \rho + \rho_a \tag{8}$$

where the over dot $(.)$ denotes differentiation with respect to t. Clearly we have two equations (6) and (7) in five unknown variables H, ρ, p, ρ_a, and p_a, where $H = \frac{\dot{a}}{a}$ is Hubble parameter, ρ is energy density and p is pressure of matter (including all the species of the universe) while ρ_a and p_a are the corresponding densities for the axion field. To obtained the exact solution of the field equations, we consider a novel generalized form of linearly varying deceleration parameter (LVDP) proposed by Akarsu and Dereli [19] that covers Berman's law indicates that the results are consistent with cosmological data. Next we consider the most general form of LVDP is given by

$$q = \frac{-\ddot{a}a}{\dot{a}^2} = -\alpha t + m - 1 \tag{9}$$

where, $\alpha \geq 0$ and $m \geq 0$ are constants. For $\alpha = 0$, equation (9) reduces to the law of Berman [20]. The sign of the deceleration parameter (DP) indicate whether the model is accelerating or decelerating. A positive sign of the DP corresponds to the standard decelerating model whereas the negative sign of the DP indicates an accelerating model. The model is inflationary for $q = 0$.

2.1. Case I $\alpha > 0$ and $m \geq 0$

For $\alpha > 0$ and $m \geq 0$ Equation (9) leads

$$a(t) = \frac{1}{1+z} = c_2 e^{\frac{2}{\sqrt{m^2 - 2\alpha c_1}} \tanh^{-1}\left(\frac{\alpha t - m}{\sqrt{m^2 - 2\alpha c_1}}\right)} \tag{10}$$

where c_1 and c_2 are constants of integration's.

Using Equation (10), the Hubble parameter (H) as

$$H(t) = \frac{2\alpha}{m^2 - 2\alpha c_1 - (\alpha t - m)^2} \tag{11}$$

The relation of scale factor and red shift is $1 + z = \frac{a_0}{a}$, where a_0 is present value of scale factor.

Deceleration parameter and Hubble parameter in terms of red shift are obtained as

$$q=\frac{-\ddot{a}a}{\dot{a}^2}=-\left[\sqrt{m^2-2\alpha c_1}\tanh\left[\frac{\sqrt{m^2-2\alpha c_1}}{2}\log\left(\frac{1}{c_2(1+z)}\right)\right]+1\right] \tag{12}$$

$$H(z)=\frac{2\alpha}{m^2-2\alpha c_1}\cosh^2\left[\frac{\sqrt{m^2-2\alpha c_1}}{2}\log\left(\frac{1}{c_2(1+z)}\right)\right] \tag{13}$$

Using Equations (6), (7) and (13); ρ_t and p_t are obtained as

$$\rho_t=\frac{1}{l_1}\left\{4\mu\left\{1+\sqrt{m^2-2\alpha c_1}\tanh\left[\frac{\sqrt{m^2-2\alpha c_1}}{2}\log\left(\frac{1}{c_2(1+z)}\right)\right]\right\}-32l_2\right\} \times\frac{\alpha^2}{\left(m^2-2\alpha c_1\right)^2}\cosh^4\left[\frac{\sqrt{m^2-2\alpha c_1}}{2}\log\left(\frac{1}{c_2(1+z)}\right)\right] \tag{14}$$

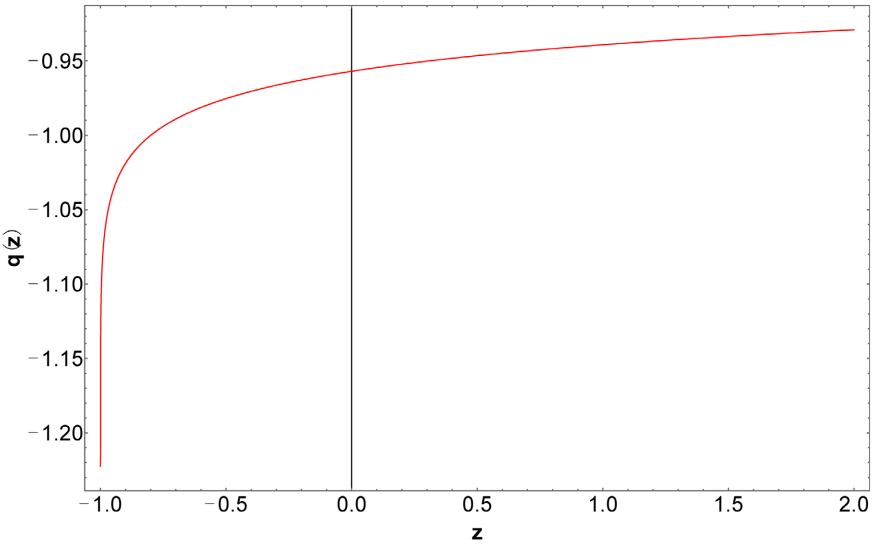

Figure 1. Plot of Deceleration parameter q *vs.* redshift z, for $\alpha=0.03$ and $m=0.01$, $c_1=-0.9$, $c_2=5$.

Figure 1 shows the graphical behaviour of deceleration parameter *q*. It should be note that for particular values of $\alpha=0.03$ and $m=0.01$, the graph of the deceleration parameter q is negative throughout the evolution of the universe. This suggest that the universe is in accelerating phase.

$$p_t=\frac{1}{8\pi+3\mu}\left\{\left(\frac{8l_2\mu}{l_1}+1\right)+\left(\frac{\mu^2}{l_1}+1\right)\left\{1+\sqrt{m^2-2\alpha c_1}\tanh\left[\frac{\sqrt{m^2-2\alpha c_1}}{2}\log\left(\frac{1}{c_2(1+z)}\right)\right]\right\}\right\} \times\frac{4\alpha^2}{\left(m^2-2\alpha c_1\right)^2}\cosh^4\left[\frac{\sqrt{m^2-2\alpha c_1}}{2}\log\left(\frac{1}{c_2(1+z)}\right)\right] \tag{15}$$

where $l_1=64\pi^2+8\mu^2+48\mu\pi$, $l_2=3\pi+\mu$.

To obtain the energy density expression from field equation we consider the following relation used by Odintsov *et al.* [21]

$$\rho_a = \overset{o}{\rho}_{dm}\, a^{-3} \tag{16}$$

where $\overset{o}{\rho}_{dm}$ is constant. Using Equations (8), (14) and (16), the energy density of the fluid is obtain as

$$\rho = \frac{1}{l_1}\left\{4\mu\left\{1+\sqrt{m^2-2\alpha c_1}\,\tanh\left[\frac{\sqrt{m^2-2\alpha c_1}}{2}\log\left(\frac{1}{c_2(1+z)}\right)\right]\right\}-32l_2\right\} \times\frac{\alpha^2}{\left(m^2-2\alpha c_1\right)^2}\cosh^4\left[\frac{\sqrt{m^2-2\alpha c_1}}{2}\log\left(\frac{1}{c_2(1+z)}\right)\right]-\overset{o}{\rho}_{dm}(1+z)^3 \tag{17}$$

Now, the barotropic EoS for the perfect fluid is defined as

$$p = \gamma\rho, \text{ where } 0 \le \gamma \le 1 \tag{18}$$

Therefore, using Equations (8), (15), (17) and (18), the pressure of axion is found to be

$$p_a = \frac{1}{8\pi+3\mu}\left\{\left(\frac{8l_2\mu}{l_1}+1\right)+\left(\frac{\mu^2}{l_1}+1\right)\left\{1+\sqrt{m^2-2\alpha c_1}\,\tanh\left[\frac{\sqrt{m^2-2\alpha c_1}}{2}\log\left(\frac{1}{c_2(1+z)}\right)\right]\right\}\right\} \times\frac{4\alpha^2}{\left(m^2-2\alpha c_1\right)^2}\cosh^4\left[\frac{\sqrt{m^2-2\alpha c_1}}{2}\log\left(\frac{1}{c_2(1+z)}\right)\right] -\frac{\gamma}{l_1}\left[4\mu\left[1+\sqrt{m^2-2\alpha c_1}\,\tanh\left(\frac{\sqrt{m^2-2\alpha c_1}}{2}\log\left(\frac{1}{c_2(1+z)}\right)\right)\right]-32l_2\right] \times\frac{\alpha^2}{\left(m^2-2\alpha c_1\right)^2}\cosh^4\left[\frac{\sqrt{m^2-2\alpha c_1}}{2}\log\left(\frac{1}{c_2(1+z)}\right)\right]+\gamma\,\overset{o}{\rho}_{dm}(1+z)^3 \tag{19}$$

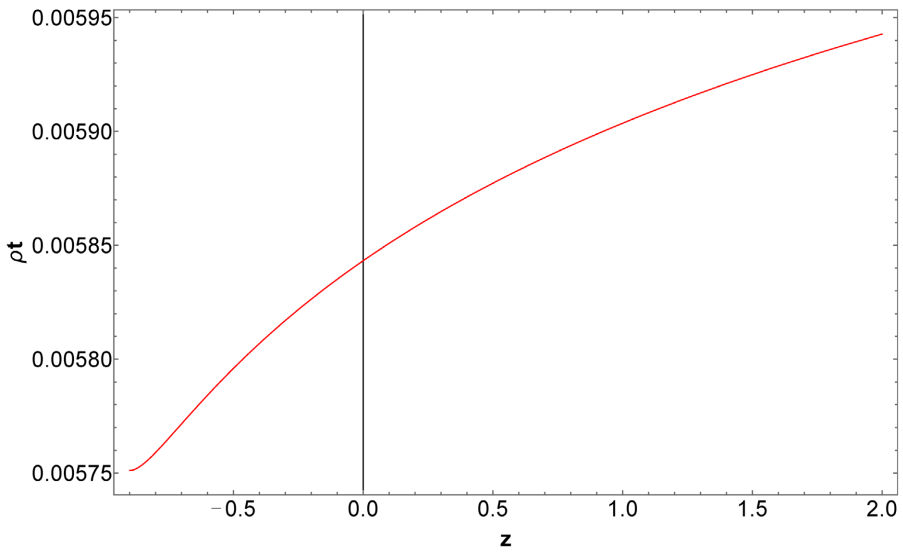

Figure 2. Plot of energy density ρ_t *vs.* redshift z of case I for $\alpha = 0.03$, $m = 0.01$, $\mu = -195$, $c_1 = -0.9$, $c_2 = 5$.

From Figure 2, it is observed that at high value of z, energy density is high and as redshift decreases the trajectory of the energy density is decreases and it is tending to zero when z tends to negative. It means that at early time of the universe density was very high as value of redshift decreases energy density decreases. When $z=0$ there is no cosmological expansion and so it seems that energy density remains constant at this point. The positive sign of z ($z>0$) indicate that the galaxies are moving away from each other i.e. the space is expanding. Larger values of z means a higher speed of the objects. Further, when the energy density is ≈0.3GeV axion like particle within the deBroglie wavelength make them oscillate coherently as a single classical field. The axion field particle maintain its coherence during the expansion of the universe [22]. Here, the plot of the energy density is linear in nature against the redshift z and its value is small, it means that axion like particle acting like single field.

The equation of state (EoS) parameter can be used to classify various epoch of the inflationary universe. The categories of various epoch of the universe depends on EoS parameter are as follows [23]:

1) **Decelerated Phases:**

- Stiff fluid if $w=1$
- Radiation dominated phase if $0<w<\frac{1}{3}$
- Dust fluid phase or cold dark matter if $w=0$

2) **Accelerated Phases:**

- The quintessence phase if $-1<w<-\frac{1}{3}$
- Cosmological constant if $w=-1$
- Phantom era if $w<-1$

The EoS parameter is defined as $w=\frac{p_t}{\rho_t}$ which is obtained as follows

$$\begin{aligned} w=&\frac{l_1}{\left\{4\mu\left\{1+\sqrt{m^2-2\alpha c_1}\tanh\left[\frac{\sqrt{m^2-2\alpha c_1}}{2}\log\left(\frac{1}{c_2(1+z)}\right)\right]\right\}-32l_2\right\}}\\ &\times\frac{\left(m^2-2\alpha c_1\right)^2}{\alpha^2\cosh^4\left[\frac{\sqrt{m^2-2\alpha c_1}}{2}\log\left(\frac{1}{c_2(1+z)}\right)\right]}\times\frac{1}{8\pi+3\mu}\left\{\left(\frac{8l_2\mu}{l_1}+1\right)\right.\\ &\left.+\left(\frac{\mu^2}{l_1}+1\right)\left\{1+\sqrt{m^2-2\alpha c_1}\tanh\left[\frac{\sqrt{m^2-2\alpha c_1}}{2}\log\left(\frac{1}{c_2(1+z)}\right)\right]\right\}\right\}\\ &\times\frac{4\alpha^2}{\left(m^2-2\alpha c_1\right)^2}\cosh^4\left[\frac{\sqrt{m^2-2\alpha c_1}}{2}\log\left(\frac{1}{c_2(1+z)}\right)\right] \end{aligned} \tag{20}$$

Figure 3 shows the graphical behaviour of EoS parameter against redshift z. It is found that when z varies from positive to negative *i.e.* from past to future

the trajectory of EoS parameter $w=\frac{p_t}{\rho_t}$ lies in the range $-1<w<-\frac{1}{3}$, which corresponds to the quintessence regime of the universe. It is important to note that for FRW spacetime in the $f(R,T)$ theory of gravitation, the EoS parameter lie in the range of phantom era [24].

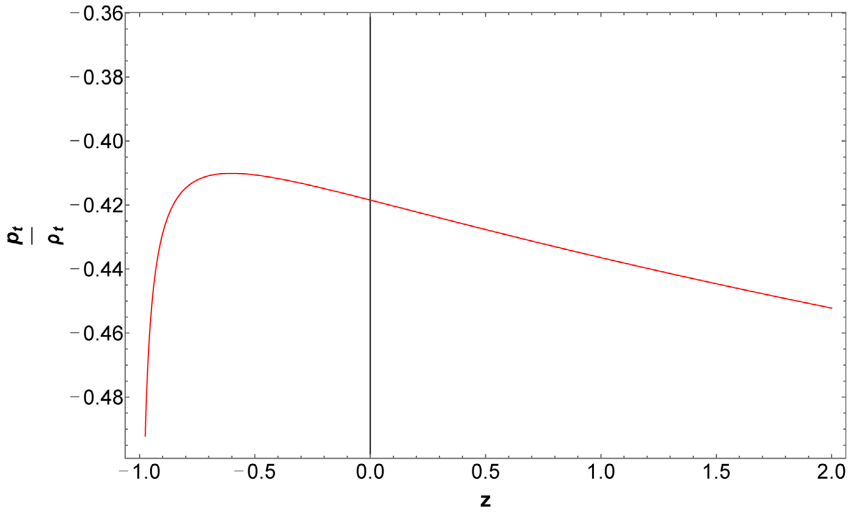

Figure 3. Plot of EoS *vs.* redshift z of case I for $\alpha=0.03$, $m=0.01$, $\mu=-195$, $c_1=-0.9$, $c_2=5$.

In the Literature, we found that, several researchers have been extensively studied the behaviour of quintessence type dark energy models in the modified theories of gravity. Caldwell *et al.* [25] first demonstrated that a cosmic fluid with a dynamically evolving EoS in the range $-1<w<-\frac{1}{3}$ can drive accelerated expansion. Subsequently, Chevallier and Polarski [26], and Linder [27] introduced a widely used parametrization of the EoS, commonly known as the CPL parametrization, to study the redshift evolution of dark energy.

The combined Type Ia supernovae and WMAP five year data at 95% confidence level place the value of EoS parameter in the range $-1.11\le w\le -0.86$ [28] whereas Type Ia supernovae, $C<B$ and 2*dfGRs* at 95% confidence level place it in the range $-1.46\le w\le -0.78$ [29]. In our model, the range of the EoS parameter is $-1\le w\le -0.4$ which is larger than the range found in observational data.

2.2. Case II for $\alpha=0$ and $m>0$

In this case, for $\alpha=0$ and $m>0$, deceleration parameter $q=m-1$ is constant and it is negative for $m<1$,thus the universe is accelerating for $m<1$. As discussed above, we have now solved the field equations by considering the deceleration parameter proposed by Akarsu and Dereli [19] in Equation (9) with $\alpha=0$ and $m>0$ leads to

$$a(t)=\left(c_3t+c_4\right)^{\frac{1}{m}} \tag{21}$$

where c_3 and c_4 are constants. Using Equation (21), the Hubble parameter (H) as

$$H(z)=\frac{c_3(1+z)^m}{m} \tag{22}$$

Using Equations (6), (7) and (22) ρ_t and p_t obtained as

$$\rho_t=\left(\frac{-4l_2+\mu(1-m)}{l_1}\right)\frac{2c_3^2(1+z)^{2m}}{m^2} \tag{23}$$

$$p_t=\frac{1}{8\pi+3\mu}\left[2\mu\left(\frac{-4l_2+\mu(1-m)}{l_1}\right)+2(1-m)+1\right]\frac{c_3^2(1+z)^{2m}}{m^2} \tag{24}$$

Using Equations (8), (16) and (23) energy density is obtained as

$$\rho=\left(\frac{-4l_2+\mu(1-m)}{l_1}\right)\frac{2c_3^2(1+z)^{2m}}{m^2}-\dot{\rho}_{dm}(1+z)^3 \tag{25}$$

Using Equation (8), (18), (24) and (25)

$$\begin{aligned}p_a=&\frac{1}{8\pi+3\mu}\left[2\mu\left(\frac{-4l_2+\mu(1-m)}{l_1}\right)+2(1-m)+1\right]\frac{c_3^2(1+z)^{2m}}{m^2}\\&-\gamma\left[\left(\frac{-4l_2+\mu(1-m)}{l_1}\right)\frac{2c_3^2(1+z)^{2m}}{m^2}-\overset{o}{\rho}_{dm}(1+z)^3\right]\end{aligned} \tag{26}$$

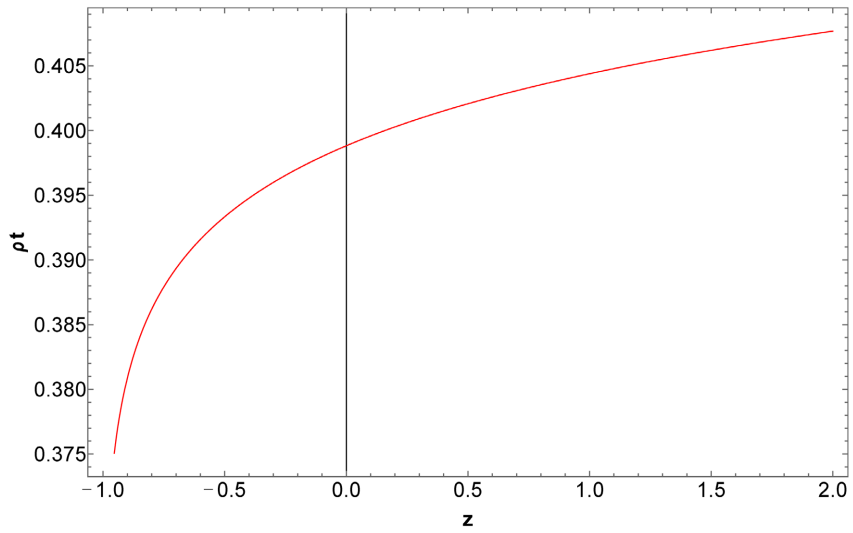

Figure 4. Plot of energy density ρ_t *vs.* redshift z of case II for $m=0.01$, $\mu=-195$, $C_3=0.1$.

From **Figure 4**, we observe the trajectory of energy density ρ_t varies with redshift z. At high value of redshift energy density is high. The energy density is decreases as value of redshift decreases. It is worth to note that the trajectories of energy density in case I and in case II are decreasing with decreasing values of redshift. However, there behavior is different which clearly indicate the effect of

parameter α.

$$w=\frac{\frac{1}{8\pi+3\mu}\left[2\mu\left(\frac{-4l_2+\mu(1-m)}{l_1}\right)+2(1-m)+1\right]\frac{c_3^2(1+z)^{2m}}{m^2}}{\left(\frac{-4l_2+\mu(1-m)}{l_1}\right)\frac{2c_3^2(1+z)^{2m}}{m^2}} \tag{27}$$

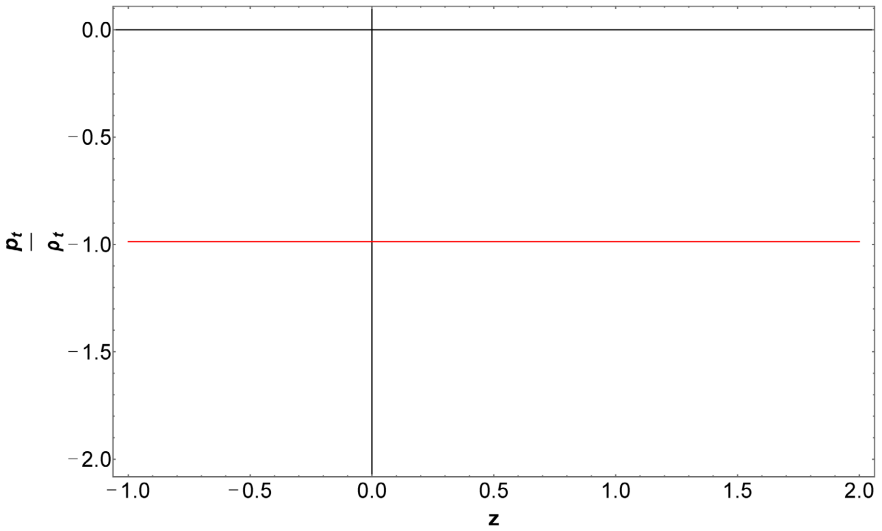

Figure 5. Plot of EoS *vs.* redshift z of case II for $m=0.01$, $\mu=-195$, $C_3=0.1$.

In **Figure 5**, diagram shows the EoS parameter w. The curve of EoS is remain constant at $w=-1$. The model represents ΛCDM model of the universe. The result is consistent with the exponential model studied by [30].

3. State Finder Pair

In cosmology, the term "statefinder pair" denotes a pair of dimensionless quantities that can be utilized to differentiate among various cosmological models in terms of the evolution of the cosmic scale factor $a(t)$ and its derivatives with time. Such parameters were proposed by Sahni *et al.* [31]. The statefinder pair $\{r,s\}$ may be estimated from observational data to investigate dark energy and the expansion of the universe. Various cosmological models, such as those with various types of dark energy or modified gravity, may yield different curves in the $\{r,s\}$ plane, which enables scientists to constrain and compare these models with observations. Ratra and Peebles [32], Kamenschik *et al.* [33], Armendariz *et al.* [34] and Dvali *et al.* [35] have investigated various studies to observe the behaviour the different DE forms, such as quintessence, Chaplygin gas, k-essence and brane world model. The statefinder parameters pair are given by:

$$r=\frac{\dddot{a}}{aH^3} \text{ and } s=\frac{r-1}{3q-\frac{3}{2}} \tag{28}$$

It is primarily invented to characterized flat universe model with cold dark mat-

ter and dark matter. When $r=1$, $s=0$, it defines cosmological constant model. Below we considered subsequently the case of $f(R,T)$ gravity. Therefore. for the case I, the Statefinder pair are obtained as

$$r=1-3m+\frac{3}{2}\left[\sqrt{m^2-2\alpha c_1}\tanh\left[\frac{\sqrt{m^2-2\alpha c_1}}{2}\log\left(\frac{1}{c_2(1+z)}\right)\right]+m\right]^2-\alpha c_1+2m^2 \quad (29)$$

$$s=\frac{-3m+\frac{3}{2}\left[\sqrt{m^2-2\alpha c_1}\tanh\left[\frac{\sqrt{m^2-2\alpha c_1}}{2}\log\left(\frac{1}{c_2(1+z)}\right)\right]+m\right]^2-\alpha c_1+2m^2}{-3\left[\sqrt{m^2-2\alpha c_1}\tanh\left[\frac{\sqrt{m^2-2\alpha c_1}}{2}\log\left(\frac{1}{c_2(1+z)}\right)\right]+1\right]-\frac{3}{2}} \quad (30)$$

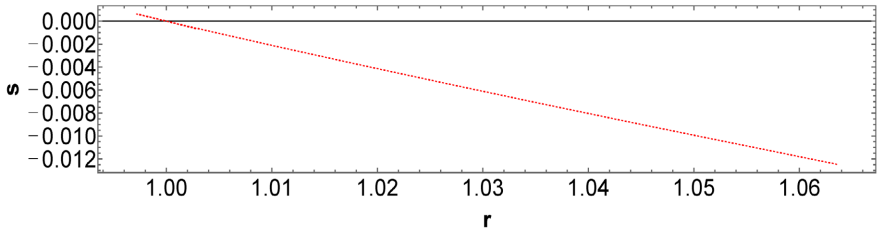

Figure 6. Plot of $\{r,s\}$ parameter of case I for $\alpha=0.03$, $m=0.01$, $c_1=-0.9$, $c_2=5$.

Figure 6 shows plot of state finder parameter. The statefinder pair $\{r,s\}$ a diagnostic tool employed to differentiate various cosmological models of dark energy.In the present cosmological model, the trajectory of r and s lies in between $0<r<1.05$ and $-0.01<s<0$. It is observed that when r near zero, s greater than zero which characterizes quintessence type dark energy. As the universe evolves, the trajectory approaches the ΛCDM fixed point $\{r,s\}=\{1,0\}$ and then moves into the region $r>1$, $s<0$ which is Chaplygin gas dominated. Therefore, initially model behaves like a quintessence universe and in future it will be Chaplygin gas dominated. Santhi *et al.* [36], Samantha and Mishra [37], Hatkar *et al.* [38] are some of the authors who have studied statefinder parameters in the present of cosmic time.

Also, for the case II, the Statefinder pair are found to be

$$r=(1-2m)(1-m) \quad (31)$$

$$s=\frac{(1-2m)(1-m)-1}{3(m-1)-\frac{3}{2}} \quad (32)$$

In case II, for $m=0.01$, $\{r,s\}$ approaches to $\{1,0\}$ that is it represent ΛCDM.

4. Energy Condition

Within the framework of general relativity and its generalizations, energy conditions are essential mathematical tools to place physical bounds on matter and

spacetime geometry. Energy conditions are inequalities based on the energy-momentum tensor and can be used to decide the feasibility of a gravitational theory. Arora *et al*. [39] explore the energy conditions in $f(Q,T)$ gravity generalized theory of gravity where in the gravitational Lagrangian is a function of the non-metricity scalar Q and the trace of the energy-momentum tensor T. The energy conditions are defined as follows:

i) Null Energy Condition (NEC): $\Leftrightarrow \rho_t + p_t \geq 0$. It ensures that energy density along light ray is non-negative.

ii) Weak Energy Condition (WEC): $\Leftrightarrow \rho_t + p_t \geq 0$ and $\rho_t \geq 0$. This indicates that the energy density is non-negative .

iii) Strong Energy Condition (SEC): $\Leftrightarrow \rho_t + p_t \geq 0$ and $\rho_t + 3p_t \geq 0$. The SEC indicates that the gravity is universally attractive. It comes into the Raychaudhuri equation and is connected with the deceleration of the universe. Violation of SEC is required for the acceleration of the universe.

iv) Dominant Energy Condition (DEC): $\Leftrightarrow \rho_t \pm p_t \geq 0$ and $\rho_t \geq 0$. The DEC does not allow energy to generate superluminally and insists that pressure is dominated by energy density.

4.1. Energy Conditions of Case I:

NEC $\Rightarrow$

$$\begin{aligned}\rho_t + p_t = \frac{1}{l_1}\Bigg\{4\mu\Bigg\{1+\sqrt{m^2-2\alpha c_1}\tanh\left[\frac{\sqrt{m^2-2\alpha c_1}}{2}\log\left(\frac{1}{c_2(1+z)}\right)\right]\Bigg\}-32l_2\Bigg\}\\ \times\frac{\alpha^2}{\left(m^2-2\alpha c_1\right)^2}\cosh^4\left[\frac{\sqrt{m^2-2\alpha c_1}}{2}\log\left(\frac{1}{c_2(1+z)}\right)\right]+\frac{1}{8\pi+3\mu}\Bigg\{\left(\frac{8l_2\mu}{l_1}+1\right)\\ +\left(\frac{\mu^2}{l_1}+1\right)\Bigg\{1+\sqrt{m^2-2\alpha c_1}\tanh\left[\frac{\sqrt{m^2-2\alpha c_1}}{2}\log\left(\frac{1}{c_2(1+z)}\right)\right]\Bigg\}\Bigg\}\\ \times\frac{4\alpha^2}{\left(m^2-2\alpha c_1\right)^2}\cosh^4\left[\frac{\sqrt{m^2-2\alpha c_1}}{2}\log\left(\frac{1}{c_2(1+z)}\right)\right]\end{aligned} \tag{33}$$

WEC $\Rightarrow$

$$\begin{aligned}\rho_t + p_t = \frac{1}{l_1}\Bigg\{4\mu\Bigg\{1+\sqrt{m^2-2\alpha c_1}\tanh\left[\frac{\sqrt{m^2-2\alpha c_1}}{2}\log\left(\frac{1}{c_2(1+z)}\right)\right]\Bigg\}-32l_2\Bigg\}\\ \times\frac{\alpha^2}{\left(m^2-2\alpha c_1\right)^2}\cosh^4\left[\frac{\sqrt{m^2-2\alpha c_1}}{2}\log\left(\frac{1}{c_2(1+z)}\right)\right]+\frac{1}{8\pi+3\mu}\Bigg\{\left(\frac{8l_2\mu}{l_1}+1\right)\\ +\left(\frac{\mu^2}{l_1}+1\right)\Bigg\{1+\sqrt{m^2-2\alpha c_1}\tanh\left[\frac{\sqrt{m^2-2\alpha c_1}}{2}\log\left(\frac{1}{c_2(1+z)}\right)\right]\Bigg\}\Bigg\}\\ \times\frac{4\alpha^2}{\left(m^2-2\alpha c_1\right)^2}\cosh^4\left[\frac{\sqrt{m^2-2\alpha c_1}}{2}\log\left(\frac{1}{c_2(1+z)}\right)\right]\end{aligned} \tag{34}$$

and

$$\rho_t=\frac{1}{l_1}\left\{4\mu\left\{1+\sqrt{m^2-2\alpha c_1}\tanh\left[\frac{\sqrt{m^2-2\alpha c_1}}{2}\log\left(\frac{1}{c_2(1+z)}\right)\right]\right\}-32l_2\right\}$$
$$\times\frac{\alpha^2}{\left(m^2-2\alpha c_1\right)^2}\cosh^4\left[\frac{\sqrt{m^2-2\alpha c_1}}{2}\log\left(\frac{1}{c_2(1+z)}\right)\right]$$

SEC $\Rightarrow$

$$\rho_t+p_t=\frac{1}{l_1}\left\{4\mu\left\{1+\sqrt{m^2-2\alpha c_1}\tanh\left[\frac{\sqrt{m^2-2\alpha c_1}}{2}\log\left(\frac{1}{c_2(1+z)}\right)\right]\right\}-32l_2\right\}$$
$$\times\frac{\alpha^2}{\left(m^2-2\alpha c_1\right)^2}\cosh^4\left[\frac{\sqrt{m^2-2\alpha c_1}}{2}\log\left(\frac{1}{c_2(1+z)}\right)\right]+\frac{1}{8\pi+3\mu}\left\{\left(\frac{8l_2\mu}{l_1}+1\right)\right.$$
$$\left.+\left(\frac{\mu^2}{l_1}+1\right)\left\{1+\sqrt{m^2-2\alpha c_1}\tanh\left[\frac{\sqrt{m^2-2\alpha c_1}}{2}\log\left(\frac{1}{c_2(1+z)}\right)\right]\right\}\right\}$$
$$\times\frac{4\alpha^2}{\left(m^2-2\alpha c_1\right)^2}\cosh^4\left[\frac{\sqrt{m^2-2\alpha c_1}}{2}\log\left(\frac{1}{c_2(1+z)}\right)\right] \tag{35}$$

and

$$\rho_t+3p_t=\frac{1}{l_1}\left\{4\mu\left\{1+\sqrt{m^2-2\alpha c_1}\tanh\left[\frac{\sqrt{m^2-2\alpha c_1}}{2}\log\left(\frac{1}{c_2(1+z)}\right)\right]\right\}-32l_2\right\}$$
$$\times\frac{\alpha^2}{\left(m^2-2\alpha c_1\right)^2}\cosh^4\left[\frac{\sqrt{m^2-2\alpha c_1}}{2}\log\left(\frac{1}{c_2(1+z)}\right)\right]+\frac{3}{8\pi+3\mu}\left\{\left(\frac{8l_2\mu}{l_1}+1\right)\right.$$
$$\left.+\left(\frac{\mu^2}{l_1}+1\right)\left\{1+\sqrt{m^2-2\alpha c_1}\tanh\left[\frac{\sqrt{m^2-2\alpha c_1}}{2}\log\left(\frac{1}{c_2(1+z)}\right)\right]\right\}\right\}$$
$$\times\frac{4\alpha^2}{\left(m^2-2\alpha c_1\right)^2}\cosh^4\left[\frac{\sqrt{m^2-2\alpha c_1}}{2}\log\left(\frac{1}{c_2(1+z)}\right)\right]$$

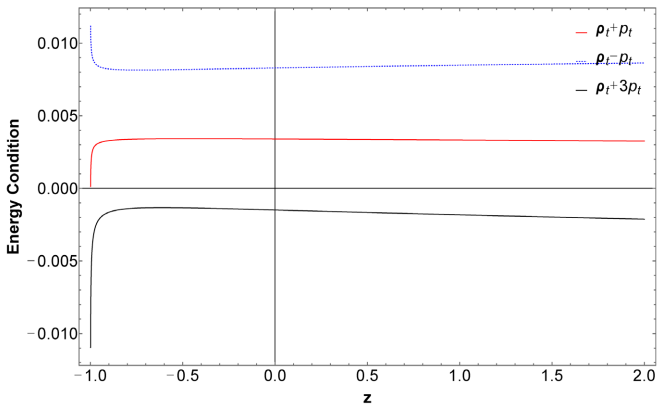

Figure 7. Plot of energy condition of case I for for $\alpha=0.03$, $m=0.01$, $\mu=-195$, $c_1=-0.9$, $c_2=5$.

Figure 7 represents graphical behavior of NEC ,WEC SEC and DEC. It is found that NEC violate in future where as SEC was violated in the past where $z>0$. Furthermore, DEC as satisfied by the model. Violation of SEC implies the acceleration phase of the universe while the violation of NEC depicts the existence of exotic matter [40]. Recent observational studies indicate that NEC and WEC are violate at large value of redshift but satisfied at small values of redshift.

DEC $\Rightarrow$

$$\begin{aligned}\rho_t+p_t=&\frac{1}{l_1}\left\{4\mu\left\{1+\sqrt{m^2-2\alpha c_1}\tanh\left[\frac{\sqrt{m^2-2\alpha c_1}}{2}\log\left(\frac{1}{c_2(1+z)}\right)\right]\right\}-32l_2\right\}\\&\times\frac{\alpha^2}{\left(m^2-2\alpha c_1\right)^2}\cosh^4\left[\frac{\sqrt{m^2-2\alpha c_1}}{2}\log\left(\frac{1}{c_2(1+z)}\right)\right]+\frac{1}{8\pi+3\mu}\left\{\left(\frac{8l_2\mu}{l_1}+1\right)\right.\\&\left.+\left(\frac{\mu^2}{l_1}+1\right)\left\{1+\sqrt{m^2-2\alpha c_1}\tanh\left[\frac{\sqrt{m^2-2\alpha c_1}}{2}\log\left(\frac{1}{c_2(1+z)}\right)\right]\right\}\right\}\\&\times\frac{4\alpha^2}{\left(m^2-2\alpha c_1\right)^2}\cosh^4\left[\frac{\sqrt{m^2-2\alpha c_1}}{2}\log\left(\frac{1}{c_2(1+z)}\right)\right]\\\rho_t-p_t=&\frac{1}{l_1}\left\{4\mu\left\{1+\sqrt{m^2-2\alpha c_1}\tanh\left[\frac{\sqrt{m^2-2\alpha c_1}}{2}\log\left(\frac{1}{c_2(1+z)}\right)\right]\right\}-32l_2\right\}\\&\times\frac{\alpha^2}{\left(m^2-2\alpha c_1\right)^2}\cosh^4\left[\frac{\sqrt{m^2-2\alpha c_1}}{2}\log\left(\frac{1}{c_2(1+z)}\right)\right]-\frac{1}{8\pi+3\mu}\left\{\left(\frac{8l_2\mu}{l_1}+1\right)\right.\\&\left.+\left(\frac{\mu^2}{l_1}+1\right)\left\{1+\sqrt{m^2-2\alpha c_1}\tanh\left[\frac{\sqrt{m^2-2\alpha c_1}}{2}\log\left(\frac{1}{c_2(1+z)}\right)\right]\right\}\right\}\\&\times\frac{4\alpha^2}{\left(m^2-2\alpha c_1\right)^2}\cosh^4\left[\frac{\sqrt{m^2-2\alpha c_1}}{2}\log\left(\frac{1}{c_2(1+z)}\right)\right]\end{aligned}\tag{36}$$

and

$$\begin{aligned}\rho_t=&\frac{1}{l_1}\left\{4\mu\left\{1+\sqrt{m^2-2\alpha c_1}\tanh\left[\frac{\sqrt{m^2-2\alpha c_1}}{2}\log\left(\frac{1}{c_2(1+z)}\right)\right]\right\}-32l_2\right\}\\&\times\frac{\alpha^2}{\left(m^2-2\alpha c_1\right)^2}\cosh^4\left[\frac{\sqrt{m^2-2\alpha c_1}}{2}\log\left(\frac{1}{c_2(1+z)}\right)\right]\end{aligned}$$

4.2. Energy Conditions of Case II:

NEC $\Rightarrow$

$$\begin{aligned}\rho_t+p_t=&\left(\frac{-4l_2+\mu(1-m)}{l_1}\right)\frac{2c_3^2(1+z)^{2m}}{m^2}\\&+\frac{1}{8\pi+3\mu}\left[2\mu\left(\frac{-4l_2+\mu(1-m)}{l_1}\right)+2(1-m)+1\right]\times\frac{c_3^2(1+z)^{2m}}{m^2}\end{aligned}\tag{37}$$

WEC $\Rightarrow$

$$\rho_t + p_t = \left(\frac{-4l_2 + \mu(1-m)}{l_1}\right)\frac{2c_3^2(1+z)^{2m}}{m^2} + \frac{1}{8\pi+3\mu}\left[2\mu\left(\frac{-4l_2+\mu(1-m)}{l_1}\right)+2(1-m)+1\right]\times\frac{c_3^2(1+z)^{2m}}{m^2} \quad (38)$$

and

$$\rho_t = \left(\frac{-4l_2 + \mu(1-m)}{l_1}\right)\frac{2c_3^2(1+z)^{2m}}{m^2}$$

SEC $\Rightarrow$

$$\rho_t + p_t = \left[2\left(\frac{-4l_2+\mu(1-m)}{l_1}\right)+\frac{1}{8\pi+3\mu}\left[2\mu\left(\frac{-4l_2+\mu(1-m)}{l_1}\right)+2(1-m)+1\right]\right]\frac{c_3^2}{m^2(c_3t+c_4)^2}$$

$$\left(\frac{-4l_2+\mu(1-m)}{l_1}\right)\frac{2c_3^2(1+z)^{2m}}{m^2}+\frac{1}{8\pi+3\mu}\left[2\mu\left(\frac{-4l_2+\mu(1-m)}{l_1}\right)+2(1-m)+1\right]\times\frac{c_3^2(1+z)^{2m}}{m^2} \quad (39)$$

and

$$\rho_t + 3p_t = \left(\frac{-4l_2+\mu(1-m)}{l_1}\right)\frac{2c_3^2(1+z)^{2m}}{m^2} + \frac{3}{8\pi+3\mu}\left[2\mu\left(\frac{-4l_2+\mu(1-m)}{l_1}\right)+2(1-m)+1\right]\times\frac{c_3^2(1+z)^{2m}}{m^2}$$

DEC $\Rightarrow$

$$\rho_t + p_t = \left(\frac{-4l_2+\mu(1-m)}{l_1}\right)\frac{2c_3^2(1+z)^{2m}}{m^2} + \frac{1}{8\pi+3\mu}\left[2\mu\left(\frac{-4l_2+\mu(1-m)}{l_1}\right)+2(1-m)+1\right]\times\frac{c_3^2(1+z)^{2m}}{m^2},$$

$$\rho_t - p_t = \left(\frac{-4l_2+\mu(1-m)}{l_1}\right)\frac{2c_3^2(1+z)^{2m}}{m^2} - \frac{1}{8\pi+3\mu}\left[2\mu\left(\frac{-4l_2+\mu(1-m)}{l_1}\right)+2(1-m)+1\right]\times\frac{c_3^2(1+z)^{2m}}{m^2} \quad (40)$$

and

$$\rho_t = \left(\frac{-4l_2+\mu(1-m)}{l_1}\right)\frac{2c_3^2(1+z)^{2m}}{m^2}$$

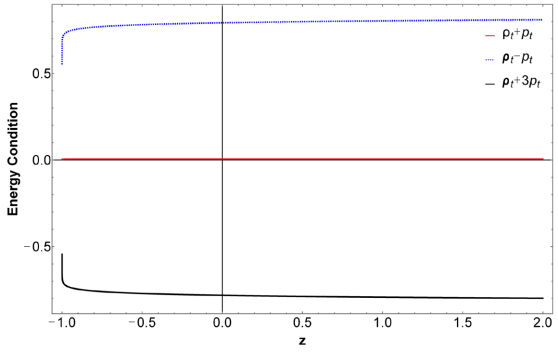

Figure 8. Plot of energy condition of Case II for $m = 0.01$, $\mu = -195$, $C_3 = 0.1$.

From Figure 8, it is observed that, the DEC is positive and SEC is negative throughout the evolution of the universe. It shows that NEC and DEC are satisfied and SEC is violated. This shows that universe is in phase of accelerated expansion.

5. Conclusion

In this work, we have studied axion dark matter in the context of $f(R,T)$ theory of gravitation. To solve the field equations, we have considered linearly varying deceleration parameter. Two different cases are investigated. In the case I, it is observed that the universe is accelerating and the rate of expansion of the universe is decreasing. The range of EoS parameter indicate that the universe is dominated by quintessence type axion dark matter. The range of EoS parameter is smaller than that found in observational data. The state finder parameter pair indicate that the universe was dominated by quintessence type axion dark matter in early era and in the future, it will be dominated by Chaplygin gas type axion dark matter. Whereas in case II, the universe is accelerating for $m<1$ and expanding. The difference in trajectories of the energy density in case I and case II may be due to constant parameter α. The universe is dominated by ΛCDM model. The DEC is satisfied and SEC is violated in both case I and case II.

Conflicts of Interest

The authors declare no conflicts of interest regarding the publication of this paper.

References

[1] Riess, A.G., Filippenko, A.V., Challis, P., Clocchiatti, A., Diercks, A., Garnavich, P.M., *et al*. (1998) Observational Evidence from Supernovae for an Accelerating Universe and a Cosmological Constant. *The Astronomical Journal*, **116**, 1009-1038. https://doi.org/10.1086/300499

[2] Perlmutter, S. and Schmidt, B.P. (2003) Measuring Cosmology with Supernovae. In: Weiler, K.W., Ed., *Supernovae and Gamma-Ray Bursters*, Springer, 195-217. https://doi.org/10.1007/3-540-45863-8_11

[3] Vishwakarma, R.G. (2002) Consequences for Some Dark Energy Candidates from the Type Ia Supernova SN 1997ff. *Monthly Notices of the Royal Astronomical Society*, **331**, 776-784. https://doi.org/10.1046/j.1365-8711.2002.05253.x

[4] Netterfield, C.B., Ade, P.A.R., Bock, J.J., Bond, J.R., Borrill, J., Boscaleri, A., *et al*. (2002) A Measurement by Boomerang of Multiple Peaks in the Angular Power Spectrum of the Cosmic Microwave Background. *The Astrophysical Journal*, **571**, 604-614. https://doi.org/10.1086/340118

[5] Buchdahl, H.A. (1970) Non-Linear Lagrangians and Cosmological Theory. *Monthly Notices of the Royal Astronomical Society*, **150**, 1-8. https://doi.org/10.1093/mnras/150.1.1

[6] De Felice, A. and Tsujikawa, S. (2010) $f(R)$ Theories. *Living Reviews in Relativity*, **13**, Article No. 3. https://doi.org/10.12942/lrr-2010-3

[7] Nojiri, S., Odintsov, S.D., Toporensky, A. and Tretyakov, P. (2010) Reconstruction and Deceleration-Acceleration Transitions in Modified Gravity. *General Relativity and Gravitation*, **42**, 1997-2008. https://doi.org/10.1007/s10714-010-0977-5

[8] Harko, T., Lobo, F.S.N., Nojiri, S. and Odintsov, S.D. (2011) $f(R,T)$ Gravity. *Physical Review D*, **84**, Article ID: 024020. https://doi.org/10.1103/physrevd.84.024020

[9] Capozziello, S., Cardone, V.F., Farajollahi, H. and Ravanpak, A. (2011) Cosmography in $f(T)$ Gravity. *Physical Review D*, **84**, Article ID: 043527. https://doi.org/10.1103/physrevd.84.043527

[10] Houndjo, M.J.S. (2012) Reconstruction of $f(R,T)$ Gravity Describing Matter Dominated and Accelerated Phases. *International Journal of Modern Physics D*, **21**, Article ID: 1250003. https://doi.org/10.1142/s0218271812500034

[11] Reddy, D.R.K., Santikumar, R. and Naidu, R.L. (2012) Bianchi Type-III Cosmological Model in $f(R,T)$ Theory of Gravity. *Astrophysics and Space Science*, **342**, 249-252. https://doi.org/10.1007/s10509-012-1158-7

[12] Moraes, P.H.R.S. (2014) Cosmology from Induced Matter Model Applied to 5D $f(R,T)$ Theory. *Astrophysics and Space Science*, **352**, 273-279. https://doi.org/10.1007/s10509-014-1895-x

[13] Azizi, T. (2013) Wormhole Geometries in $f(R,T)$ Gravity. *International Journal of Theoretical Physics*, **52**, 3486-3493. https://doi.org/10.1007/s10773-013-1650-z

[14] Elizalde, E. and Khurshudyan, M. (2019) Wormhole Models in $f(R,T)$ Gravity. *International Journal of Modern Physics D*, **28**, Article ID: 1950172. https://doi.org/10.1142/s0218271819501724

[15] Banerjee, A., Jasim, M.K. and Ghosh, S.G. (2021) Wormholes in $f(R,T)$ Gravity Satisfying the Null Energy Condition with Isotropic Pressure. *Annals of Physics*, **433**, Article ID: 168575. https://doi.org/10.1016/j.aop.2021.168575

[16] Pradhan, A., Maurya, D.C. and Dixit, A. (2021) Dark Energy Nature of Viscus Universe in $f(Q)$-Gravity with Observational Constraints. *International Journal of Geometric Methods in Modern Physics*, **18**, Article ID: 2150124. https://doi.org/10.1142/s0219887821501243

[17] Bertolami, O., Böhmer, C.G., Harko, T. and Lobo, F.S.N. (2007) Extra Force in $f(R)$ Modified Theories of Gravity. *Physical Review D*, **75**, Article ID: 104016. https://doi.org/10.1103/physrevd.75.104016

[18] Singh, C.P. and Singh, V. (2014) Reconstruction of Modified $f(R,T)$ Gravity with Perfect Fluid Cosmological Models. *General Relativity and Gravitation*, **46**, Article No. 1696. https://doi.org/10.1007/s10714-014-1696-0

[19] Akarsu, Ö. and Dereli, T. (2011) Cosmological Models with Linearly Varying Deceleration Parameter. *International Journal of Theoretical Physics*, **51**, 612-621. https://doi.org/10.1007/s10773-011-0941-5

[20] Kumar, S. and Singh, C.P. (2007) Anisotropic Bianchi Type-I Models with Constant Deceleration Parameter in General Relativity. *Astrophysics and Space Science*, **312**, 57-62. https://doi.org/10.1007/s10509-007-9623-4

[21] Odintsov, S.D., Gómez, D.S.-C. and Sharov, G.S. (2023) Exponential $f(R)$ Gravity with Axion Dark Matter. *Physics of the Dark Universe*, **42**, Article ID: 101369.

[22] Huang, G. and Nath, N. (2018) Neutrinophilic Axion-Like Dark Matter. *The European Physical Journal C*, **78**, Article No. 922. https://doi.org/10.1140/epjc/s10052-018-6391-y

[23] Santhi, M.V., Chinnappalanaidu, T., Madhu, S.S. and Gusu, D.M. (2022) Some Bianchi Type Viscous Holographic Dark Energy Cosmological Models in the Brans-Dicke

Theory. *Advances in Astronomy*, **2022**, Article ID: 5364541. https://doi.org/10.1155/2022/5364541

[24] Myrzakulov, R. (2012) FRW Cosmology in $F(R,T)$ Gravity. *The European Physical Journal C*, **72**, Article No. 2203. https://doi.org/10.1140/epjc/s10052-012-2203-y

[25] Caldwell, R.R., Dave, R. and Steinhardt, P.J. (1998) Cosmological Imprint of an Energy Component with General Equation of State. *Physical Review Letters*, **80**, 1582-1585. https://doi.org/10.1103/physrevlett.80.1582

[26] Chevallier, M. and Polarski, D. (2001) Accelerating Universes with Scaling Dark Matter. *International Journal of Modern Physics D*, **10**, 213-223. https://doi.org/10.1142/s0218271801000822

[27] Linder, E.V. (2003) Exploring the Expansion History of the Universe. *Physical Review Letters*, **90**, Article ID: 091301. https://doi.org/10.1103/physrevlett.90.091301

[28] Riess, A.G., Strolger, L., Tonry, J., Casertano, S., Ferguson, H.C., Mobasher, B., *et al*. (2004) Type Ia Supernova Discoveries at $z>1$ from the Hubble Space Telescope: Evidence for Past Deceleration and Constraints on Dark Energy Evolution. *The Astrophysical Journal*, **607**, 665-687. https://doi.org/10.1086/383612

[29] Hinshaw, G., Weiland, J.L., Hill, R.S., Odegard, N., Larson, D., Bennett, C.L., *et al*. (2009) Five-Year Wilkinson Microwave Anisotropy Probe Observations: Data Processing, Sky Maps, and Basic Results. *The Astrophysical Journal Supplement Series*, **180**, 225-245. https://doi.org/10.1088/0067-0049/180/2/225

[30] Akarsu, Ö. and Kılınç, C.B. (2010) De Sitter Expansion with Anisotropic Fluid in Bianchi Type-I Spacetime. *Astrophysics and Space Science*, **326**, 315-322. https://doi.org/10.1007/s10509-009-0254-9

[31] Sahni, V., Saini, T.D., Starobinsky, A.A. and Alam, U. (2003) Statefinder—A New Geometrical Diagnostic of Dark Energy. *Journal of Experimental and Theoretical Physics Letters*, **77**, 201-206. https://doi.org/10.1134/1.1574831

[32] Ratra, B. and Peebles, P.J.E. (1988) Cosmological Consequences of a Rolling Homogeneous Scalar Field. *Physical Review D*, **37**, 3406-3427. https://doi.org/10.1103/physrevd.37.3406

[33] Kamenshchik, A., Moschella, U. and Pasquier, V. (2001) An Alternative to Quintessence. *Physics Letters B*, **511**, 265-268. https://doi.org/10.1016/s0370-2693(01)00571-8

[34] Armendariz-Picon, C., Mukhanov, V. and Steinhardt, P.J. (2000) Dynamical Solution to the Problem of a Small Cosmological Constant and Late-Time Cosmic Acceleration. *Physical Review Letters*, **85**, 4438-4441. https://doi.org/10.1103/physrevlett.85.4438

[35] Dvali, G., Gabadadze, G. and Porrati, M. (2000) 4D Gravity on a Brane in 5D Minkowski Space. *Physics Letters B*, **485**, 208-214. https://doi.org/10.1016/s0370-2693(00)00669-9

[36] Vijaya Santhi, M., Rao, V. and Aditya, Y. (2016) Kaluza-Klein Cosmological Models with Two Fluids Source in Brans-Dicke Theory of Gravitation. *The African Review of Physics*, **11**, 227-238.

[37] Samanta, G.C. and Mishra, B. (2017) Anisotropic Cosmological Model in Presence of Holographic Dark Energy and Quintessence. *Iranian Journal of Science and Technology, Transactions A: Science*, **41**, 535-541. https://doi.org/10.1007/s40995-017-0263-4

[38] Hatkar, S.P., Karhale, G.D., Tadas, D.P., Katore, S.D. and Pawar, D.D. (2025) Homogeneous Hypersurface with Viscous Dark Energy in Lyra Geometry and $f(R,T)$

Gravity. *Annals of Physics*, **476**, Article ID: 169959. https://doi.org/10.1016/j.aop.2025.169959

[39] Arora, S., Santos, J.R.L. and Sahoo, P.K. (2021) Constraining $f(Q,T)$ Gravity from Energy Conditions. *Physics of the Dark Universe*, **31**, Article ID: 100790. https://doi.org/10.1016/j.dark.2021.100790

[40] Hassan, Z., Mustafa, G. and Sahoo, P.K. (2021) Wormhole Solutions in Symmetric Teleparallel Gravity with Noncommutative Geometry. *Symmetry*, **13**, Article No. 1260. https://doi.org/10.3390/sym13071260